Remarks on Dissociative Anion Potential Energy Curves for Organic Electron Transfers

Rudolph A. Marcus

Noyes Chemical Laboratory 127-72, California Institute of Technology, Pasadena, CA 91125, USA

Dedicated to Professor Lennart Eberson on the occasion of his 65th birthday

Marcus, R. A., 1998. Remarks on Dissociative Anion Potential Energy Curves for Organic Electron Transfers. – Acta Chem. Scand. 52: 858–863. © Acta Chemica Scandinavica 1998.

Data on electron-molecule collisions in the gas phase have been used to obtain information on the potential energy curve for the dissociation of a transient anion RX'—, where R is frequently an organic group and X often a halide. The data include thermal dissociative attachment energies and vertical attachment energies of RX. The data also consist of collision cross-sections (elastic, inelastic and dissociative) which vary with the energy of the incident electron and with the vibrational state or temperature of the molecule. Relevant expressions are discussed. An approximate temperature-dependent expression is given for the thermal dissociative attachment cross-section. The potential energy curve of the transient anion appears in the theory of electron transfer reactions of RX that are accompanied by the bond rupture of R—X.

It is a real pleasure to contribute to these special papers honoring our colleague, Professor Lennart Eberson. His major contributions to the interpretation and understanding of organic electron transfer reactions have served as a stimulating and important bridge between the organic and chemical physics communities.

Many of these electron transfer-related reactions are of the S_N2 type, $^{1-4}$ such as eqns. (1) and (2), where the A^- can also denote, instead, a cation, R is an organic group, and X^- is frequently a halide or some other anion. Reaction (1) is followed by reactions of AR.

$$A^{-} + RX \rightarrow AR^{+} + X^{-} \tag{1}$$

$$A^- + RX \rightarrow AR + X^- \tag{2}$$

Competing with these reactions are the bond dissociative electron transfers, probably largely 'outer sphere', $^{1-4}$ [eqns. (3) and (4)], followed by reactions of the resulting free radicals. In these reactions and in two-state models for the S_N2 reactions (1) and (2) a knowledge of the potential energy curve for the anion RX^{*-} is needed.

$$A^{-} + RX \rightarrow R^{+} + X^{-} \tag{3}$$

$$A^- + RX \rightarrow A^{\cdot} + R^{\cdot} + X^- \tag{4}$$

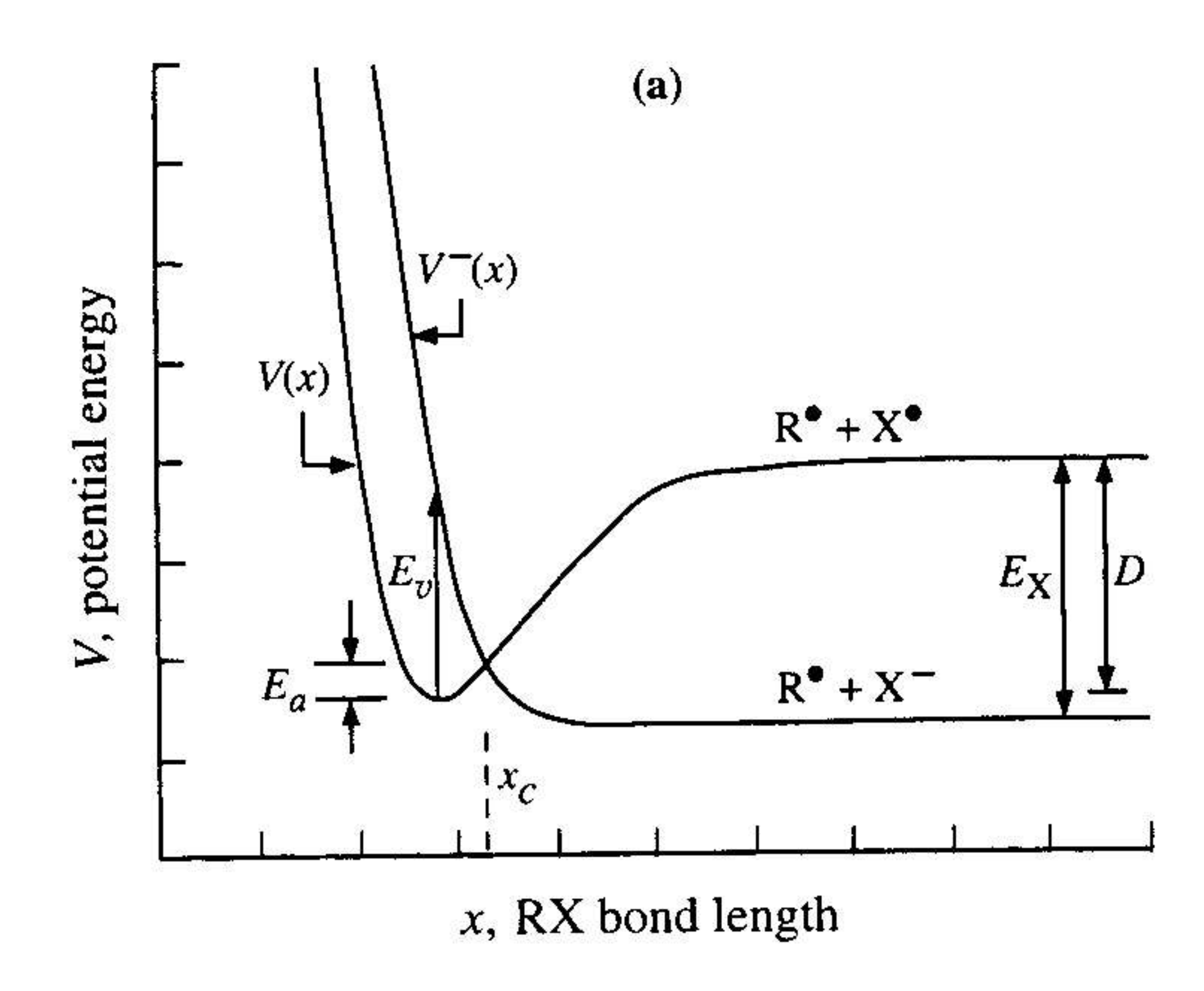
In the present paper we consider information that can be inferred about these anion potential energy curves from data on electron-molecule collisions, eqn. (5).

$$e + RX \rightarrow RX^{-} \rightarrow R' + X^{-}$$
 (5)

These data include the vertical electron attachment

energy $E_{\rm v}$, the activation energy $E_{\rm a}$ for the thermal dissociative attachment, and various electron-molecule collision cross-sections. The cross-sections are functions of the incident electron energy and of the vibrational quantum state or temperature of the molecule. These data help characterize the dissociative anion potential energy curve, though each brings with it additional factors that need to be determined also. As an overview we touch upon several of these measurements in the present article, and leave a more detailed discussion to a future contribution. A number of reviews on electronmolecule collisions are available.⁵⁻⁹ Once a gas phase anion potential energy curve has been determined for reaction(5), the modification due to the solvent in reactions (3) and (4) would still, of course, need to be considered.

Potential energy curves. The potential energy curves employed in discussion of electron-molecule collisions are of several types. One example of a potential energy curve as a function of the R-X separation distance x is given in Fig. 1(a). In that figure the RX potential energy curve $V^-(x)$ is largely repulsive, with perhaps a relatively shallow minimum, and is such that passage past the intersection $x = x_c$ with the RX curve leads either to reflection or to the dissociated products R and X. There may be more than one nearby RX potential energy curve $V^-(x)$, one such example being that in Fig. 1(b), the second curve there leading asymptotically



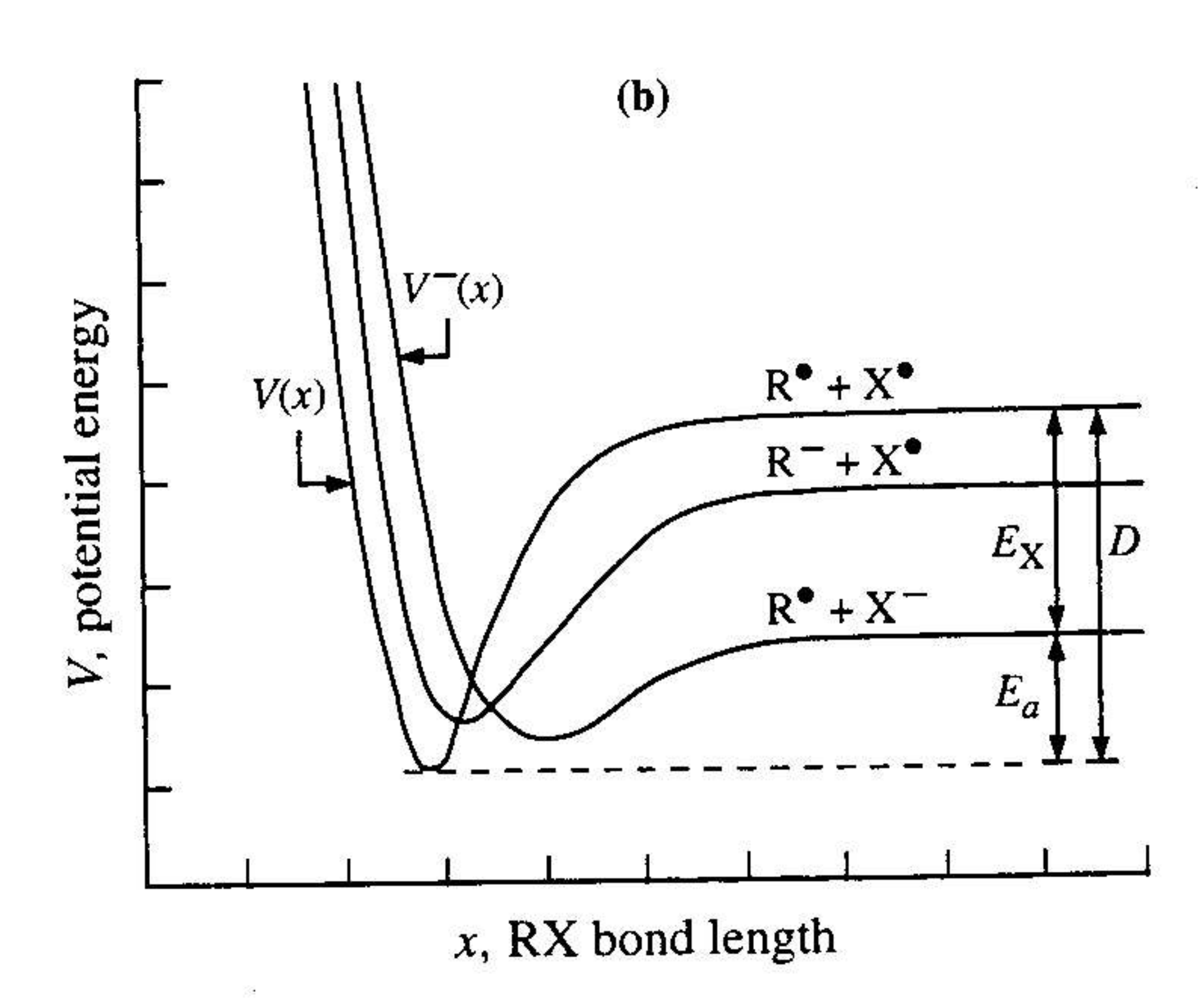


Fig. 1. Plots of potential energy curves for two cases of reaction (5). In Fig. 1(a) there is only the anion repulsive state. In Fig. 1(b) there is also an extra anion state, one which leads asymptotically to R⁻ and X⁻ instead of to R⁻ and X⁻.

to R^- and to X'. Experimentally these two cases in Fig. 1 differ notably in their relationship of E_a to other properties, as discussed later.

For purposes of the present discussion we focus on the two cases in Fig. 1. For the potential energy curve V_{RX} for RX as a function of the RX bond distance x a Morse curve will be assumed, eqn. (6), where x_0 is the equilibrium value of x in the RX molecule. For the anion in Fig. 1a a repulsive type of Morse curve $V^-(x)$ will be assumed. For the moment we write it as eqn. (7), where E_X is the electron affinity of X'. There is also in the gas phase a long-range charge-induced dipole and in some cases a charge-permanent dipole attractive term. We return later to an attractive term for $V^-(x)$.

$$V(x) = D(1 - e^{-a(x - x_o)})^2 - D$$
 (6)

$$V^{-}(x) = D^{-}e^{-2a(x-x_{o})} - E_{X}$$
 (7)

Vertical attachment energy. The vertical attachment energy $E_{\rm v}$ can be used to obtain information on $V^-(x_{\rm o})$ and, knowing $V(x_{\rm o})$, can be used to test theoretical ideas on the activation energy of reaction (3) or (4). From eqns. (6) and (7) $E_{\rm v}$ is given by eqn. (8). Experimental

values of $E_{\rm v}$ are given in Table 1 for several compounds of interest, and we use them to estimate D^- .

$$E_{v} = V^{-}(x_{o}) - V(x_{o}) = D^{-} + D - E_{X}$$
 (8)

Using for the moment the simple form of the potential energy curves given by eqns. (6) and (7), the value of D^- is immediately obtained from eqn. (8) and the known $E_{\rm v}$, D and $E_{\rm x}$. The results are given in Table 1. One approximation, which has sometimes been used in the literature, 10 is to set $D^- = D$. It is seen in Table 1 that that approximation is reasonably good for CH₃Cl and CH₃Br, but not so for the other alkyl compounds. The alkyl R groups containing more than one C have a much lower E_{v} , and hence a much lower D^{-} , than for R being CH_3 , even though the D is approximately the same. The origin of this difference is presently not known, though one suggestion 17 is that the σ^* CC orbitals in RX' depress the energy of the σ^* CX' orbital. Further theoretical work on understanding these very low $D^$ values is clearly needed.

In addition to the vertical attachment energy there is also the thermal dissociative attachment energy (DAE). For a molecule whose vibrational quantum states are thermally distributed at a temperature T, the DAE is typically shifted to lower electron energies relative to the vertical attachment energy (VAE): 17 a competition, after the initial electron attachment, occurs between the re-emission of the electron and the reaching of the intersection region x_c . Systems formed by a vertical attachment closer to the intersection, i.e., at larger RX bond amplitudes, have a greater chance of surviving the competition of the re-emission. Since they have a smaller value of $V^{-}(x) - V(x)$, they are formed at lower electron energies. Thereby, the DAE is shifted to electron energies lower than the VAE. The $E_{\rm v}$ s in Table 1 refer mainly to the VAEs of elastic or slightly inelastic collisions, and not to DAEs. We turn next to thermal activation energies E_a for the electron-molecule dissociative attachment reaction (5), where both the energy of the molecule and that of the electron are distributed thermally.

Thermal activation energy. The data on activation energies for thermal electron dissociative attachment⁹ fall more or less into two classes: in one class of reactions the activation energy is approximately equal to $D-E_{\rm X}$. In this case an interpretation⁹ is that there are two RX'states, as in Fig. 1(b), one with the charge centered on the R (typically when R is an aromatic) and the other with the charge centered on the X. For C₆H₅Cl, for example, an initial vertical attachment to form the first state then leads, after a crossing of an intersection, to the second anionic state. When both intersections are lower in energy than the asymptote of the $R'+X^-$ curve, the rate-determining transition state is somewhere along or near that asymptote. Thus, for this class, we can understand from Fig. 1(b) why their E_a values are approximately equal to $D-E_{\rm X}$.

In a second class of reactions, those in Fig. 1(a), the

Table 1. Experimental data on E_v , E_a , D, E_X^a

Entry No.	R-X	E _v	E _a	D	E _X	D -	Ref. (<i>E</i> _v)	
1	CH ₃ F	ca. 6.3		4.68	3.38	ca. 5.0	11	
2	CH ₃ CI	3.5	0.54	3.59	3.62	3.53	12, 13	
3	t-C4H9Cl	1.80	0.47	3.58	3.62	1.84	14	
4	C2H4CI-CI		0.38	3.46	3.62			
5	CH ₂ CI-CI	1.23	0.33	3.44	3.62	1.41	12	
6	CF ₂ CI-CI	2004021	0.15	3.30	3.62			
7	CHCI ₂ -CI	0.35	0.14	3.30	3.62	0.67	12	
8	CFCI ₂ -CI		0	3.17	3.62			
9	CCI3-CI	≈0	0	3.08	3.62		12	
10	CH ₃ Br	2.4	0.25	3.02	3.37	2.75	15	
11	C ₂ H ₅ Br	1.26					15	
12	n-C ₃ H ₇ Br	1.20	0.34	3.14	3.57	1.43	15	
13	CH ₂ Br–Br		0.05	2.97	3.57			
14	CHBr ₂ -Br		0.01	2.84	3.57			
15	CH ₃ I		0.03	2.45	3.06			
16	C ₂ H ₅ I	0.50	0.05	2.39	3.06	1.17	15	
17	n-C ₃ H ₇ I	0.53	\$250.05(4575004,000		3.06		15	

^aThe energies are given in eV. The D and E_X values are taken from the collection in Ref. 9, apart from CH₃F not given there, and taken from Ref. 3 (p. 165). The E_a values were taken from collection in Ref. 9. D^- is calculated from eqn. (8), using the values of E_V , D and E_X . E_V values of other RXs are given in Refs. 12, 14, 16 and 17.

activation energy $E_{\rm a}$ exceeds the difference $D-E_{\rm X}$, and the intersection of V(x) and $V^-(x)$ is higher than the asymptote of the $V^-(x)$. We focus on this more challenging class in the present paper. Some thermal activation energies $E_{\rm a}$ for the electron-molecule dissociative attachment reaction (5) for this class are tabulated in Table 1 and are plotted vs. $E_{\rm X}-D$ in Fig. 2.

The slope of the plot in Fig. 2 is approximately -1 for values of $E_{\rm X}-D$ less than 11 kcal mol⁻¹. We may compare the results in Fig. 2 with those obtained from a model for reaction (3) or (4) sometimes employed in the literature, ¹⁰ in which $D^- = D$. The value of $E_{\rm a}$ equals the value of V, $V(x_{\rm c})$, at the intersection, less the initial value $V(x_{\rm o})$. Obtaining $x_{\rm c}$ by equating $V(x_{\rm c})$ and $V^-(x_{\rm c})$, eqns.

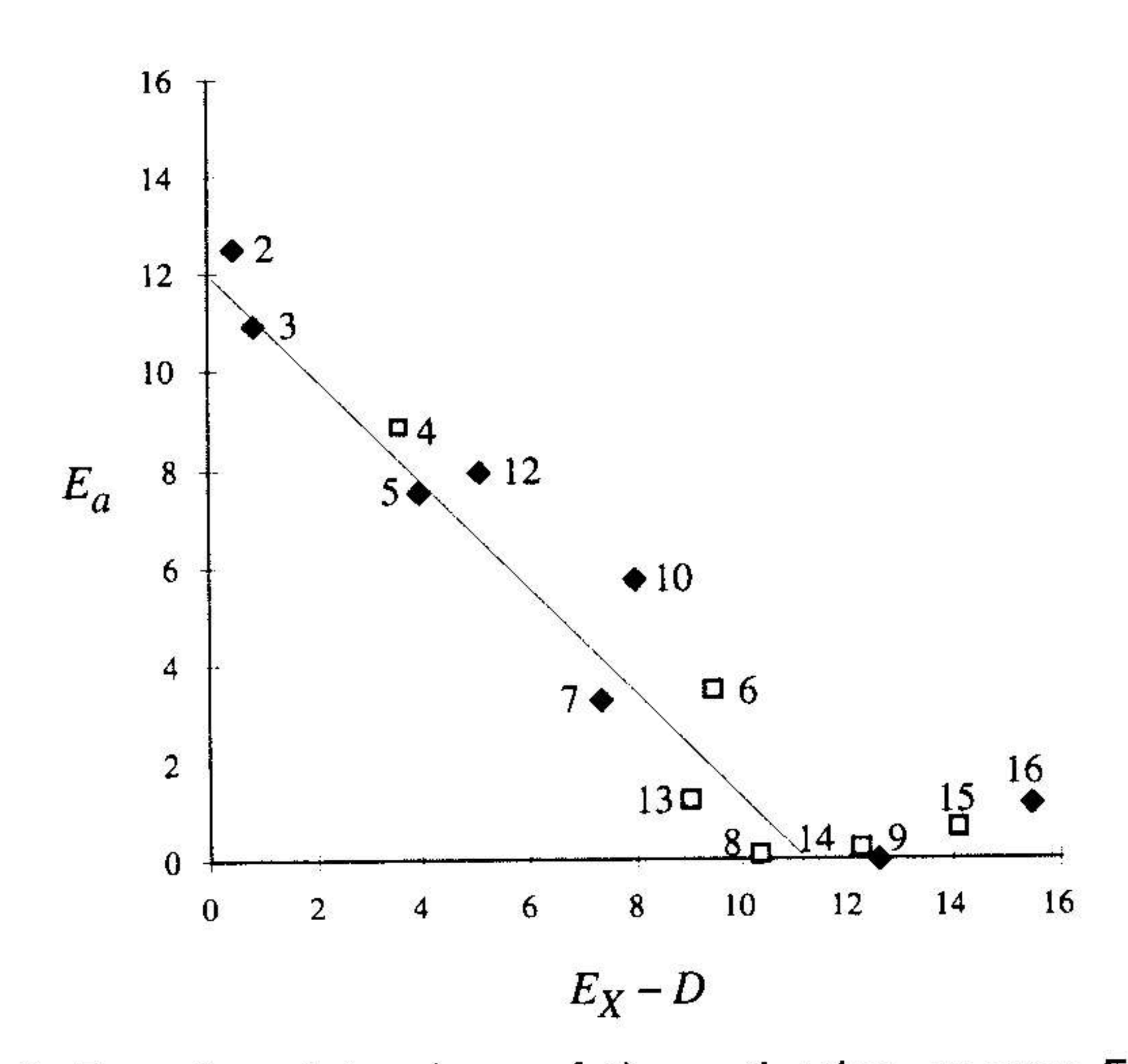


Fig. 2. Experimental values of the activation energy E_a for the thermal dissociative attachment reaction eqn. (5) plotted versus the difference E_X-D in election affinity of X and the RX dissociation energy D. The numbers beside each point refer to those in Table 1. The empty squares are points for which E_v is not available.

(6) and (7), yield, after a change of variable to X, $\{X = \exp[-a(x-x_o)]\}$, the value X_c for X at the intersection, namely $E_X/2D$. Thereby, eqn. (9) holds,

$$E_{\mathbf{a}} = D - E_{\mathbf{X}} + E_{\mathbf{X}}^2 / 4D - \Delta(\Sigma \omega \nu / 2) \tag{9}$$

where we have also subtracted the total zero-point energy of RX at x_0 minus that at x_0 . This latter difference might be of the order of 3 or so kcal mol⁻¹, depending upon the system.

If $E_{\rm X}^2/4D$ in eqn. (9) were approximately constant (which it isn't) this equation would have the roughly correct slope of -1 for the plot in Fig. 2. However, the barrier calculated from eqn. (9) is too high. For example, in the units of Fig. 2 (kcal mol⁻¹), the $E_{\rm a}$ calculated from eqn. (9) at $E_{\rm X}-D=11$ would be about 16 (or perhaps about 13 if the zero-point term were included), instead of the zero found in Fig. 2.

This breakdown of eqn. (9) is not surprising, and could have been anticipated, since in eqn. (8) the approximation of $D^- = D$ already led to incorrect values for E_v , except for CH₃Cl and CH₃Br. (For them, as seen in Table 1, $D^- \approx D$.) The use of eqn. (9) leads for CH₃Cl to a calculated E_a of 0.86 eV minus the zero-point term. (D was taken to be the mean of D and D^- in Table 1.) This calculated value is not very far from the experimental E_a of 0.54 eV, though is too high.

There are possible ways of modifying the equations for V(x) and $V^-(x)$. There is a long-range attractive term in V(x) due to an electron-molecular polarizability interaction, and also an attractive term in $V^-(x)$, at least at larger RX distances, due to the interaction of the X^- with the polarizable R. To take account of the second attractive term one could add a suitable attractive term in eqn. (7), varying as $1/r^4$ when r isn't small, where r is the distance between X^- and the polarizability center of R. One simple way of introducing some attractive term

into $V^{-}(x)$, albeit not of the correct functional form, is to set¹⁸

$$V^{-}(x) \cong D^{-}[-ce^{-b(x-x_{o})} + (1+c)e^{-2d(x-x_{o})}] - E_{X}$$
(10)

where c is a positive constant, and vanishes for a purely repulsive curve. The presence of c in eqn. (10) does not affect the evaluation of D^- from E_v , since the c terms cancel at $x = x_o$, but it does affect the calculation of E_a . Purely for economy of parameters in the present article we set b = d = a in eqns. (7) and (10) and inquire whether there is some value of c which could, in this overly simplified model, reconcile the data. Calculations with a value of c = 0.6 yield the results given in Table 2 and Fig. 3. It is seen, rather surprisingly, that this approximation provides a reasonable reconciliation of the experimental values of E_a with those of D and E_v .

Equation (10) for $V^-(x)$ displays a small potential energy well: minimizing $V^-(x)$ with respect to X yields a value of $c^2D^-/4(1+c)$ for the well depth. With a $c\approx 0.6$, this depth is seen to be about $0.056D^-$ and so, with a typical D^- of ca. 1 eV, it is only about 0.056 eV or about 1.3 kcal mol⁻¹, which is not unreasonable.

Table 2. Experimental and calculated E_a values using c=0.6 and eqns. (6) and (10)^a

Entry No.	R-X	E a obs	E a lc
2	CH ₃ Cl	0.54	0.64
3	t-C4H9CI	0.47	0.46
5	CH ₂ CĬ-CI	0.33	0.32
7	CHCI ₂ -CI	0.14	0.09
10	CH ₃ Br	0.25	0.39
12	n-C₃H ₇ Br	0.34	0.30
16	C_2H_5I	0.05	0.06

^aThe energies are given in eV. In the calculated E_a values the zero-point energy term similar to the one in eqn. (9) is omitted for brevity. If it were included, a somewhat smaller c would be used in obtaining a fit to $E_a^{\rm obs}$.

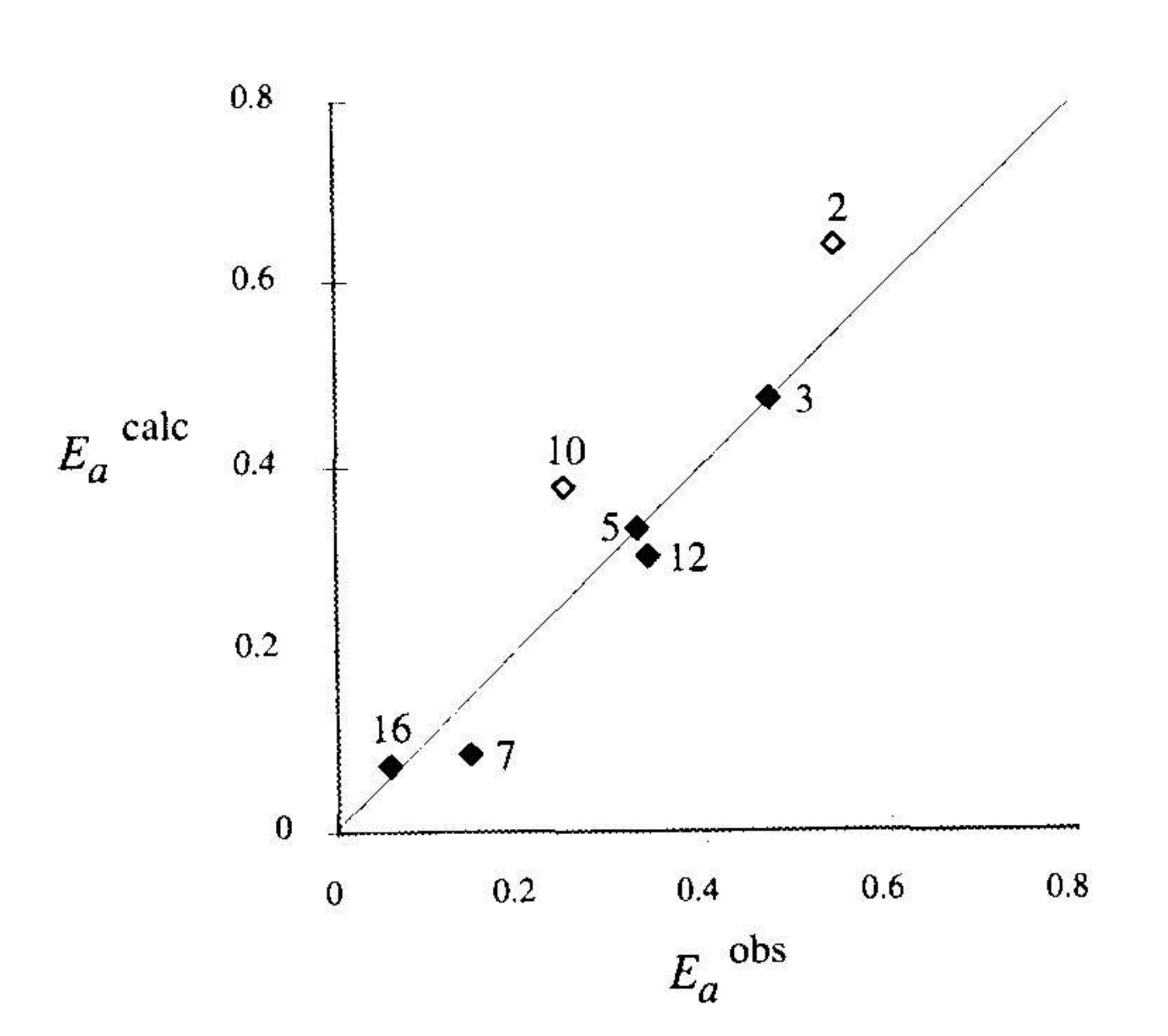


Fig. 3. Comparison of calculated and experimental E_a values. The calculated one is based on eqns. (6) and (10) with c=0.6. The numbers beside each point refer to those in Table 2. The empty diamonds are points for which the molecules are CH_3X .

However, detailed *ab initio* calculations of $V^-(x)$ are clearly desirable. In eqn. (10) the use of some average c instead of one which varies with R and with X^- is crude and does not take into account (if the origin of the attraction were mainly ion-induced dipole) the fact that the radicals differ in their polarizability. Nevertheless, the very large effect on E_a of including a small attractive term in the anion potential energy curve is striking. It will be interesting to explore its role using subsequent *ab initio* calculations of the anion potential energy curve. Of particular interest in these $V^-(x)$ curves is understanding the very large differences in the VAEs, E_v , of methyl vs. the other alkyl halides.

We turn next to a somewhat more formidable topic, the dynamics of electron-molecule collisions, an area for which there is already an extensive literature, a few of the numerous examples being Refs. 5–8, 12 and 19–47.

Cross-sections for electron-molecule collisions. It may be recalled that a collision or reaction cross-section σ is defined as the total outgoing flux of the particles from a scattering event per unit incident flux per unit area. ^{36,37} In electron-molecule collisions, the cross-sections σ for inelastic or dissociative scattering are obtained by summing over all orbital angular momentum states l of the incident electron (usually $l \approx 0$ or 1 at the typical electron energies studied in the systems of interest here) as given in eqn. (11), where P_l is the probability of the event at the given l, and k is the wavenumber for the colliding electron. The electron energy ε equals $k^2\hbar^2/2m$, where m is the electron mass.

$$\sigma = \frac{\pi}{k^2} \sum_{0}^{\infty} (2l+1) P_l \tag{11}$$

A rate constant $k(\varepsilon, n)$ for a given vibrational state n of the molecule and a given electron energy ε is $v\sigma(\varepsilon, n)$, v being the electron velocity. To calculate the overall rate constant at fixed ε this $k(\varepsilon, n)$ is then thermally averaged over the vibrational quantum states n of the molecule. Thereby, $k(\varepsilon, T)$ at a temperature T of the molecule is obtained and can be compared with data on this quantity.

If only a single resonance state of the electron–molecule system occurred, with no other source of broadening, the total cross-section σ would be^{37,38} of the Breit–Wigner form, eqn. (12), where ε_0 is the energy of the center of the resonance, and Γ is the width of the resonance at half-height. The lifetime for re-emission of the electron from this metastable resonance state is \hbar/Γ . According to an expression of Wigner³⁹ $\Gamma(\varepsilon)$ varies as $\varepsilon^{l+1/2}$. In addition to the purely resonant scattering [eqn. (12)] there may also be a background scattering of the electron. The amplitude of this background and that of the resonance can interfere, yielding a Fano lineshape expression. Further, the resonance may be pronounced at some scattering angles Ω (in a study of differential scattering cross-sections $d\sigma/d\Omega$ rather than

total cross-sections σ) and hardly visible at others, e.g., as in Ref. 13.

$$\sigma = \frac{4\pi(2l+1)}{k^2} \frac{\Gamma^2}{(\varepsilon - \varepsilon_0)^2 + (\Gamma/2)^2}$$
(12)

We consider now the dissociative attachment cross-section σ_{DA} and the inelastic cross-section for vibrational excitation of the molecule σ_n . Each σ is sensitive to the anion potential energy curve $V^-(x)$ and serves to provide further indirect experimental information about the latter, when V(x) is known, e.g. Refs. 5, 20, 21, 24, 25, 31–35, 41–47. Calculations of these σ values have been made using *ab initio* or empirical values for $V^-(x)$, most frequently for diatomic molecules. The parameters in the empirical $V^-(x)$ are chosen so as to obtain the best fit for one or both σ values.

As an illustration we consider a theoretical expression for $\sigma_{DA}(\varepsilon, n)$ that is based on the Franck-Condon principle, and indicate a simple approximate extension when the molecule has a thermal equilibrium distribution of n at a temperature T, rather than being only in a preselected vibrational state n.

Apart from various constants, omitted here in the interests of notational brevity, σ_{DA} is given, with several approximations, as a function of the energy ε of the incident electron and of the vibrational state n of the molecule by eqn. (13), 19,21,22 where χ_n is the initial vibrational wavefunction of the molecule, x_{ε} is the value of x which satisfies the Franck-Condon restriction in eqn. (14) for the attachment of an electron of energy ε , $\Gamma(x_{\varepsilon})/\hbar$ is the autoionization rate of the electron in the anion at $x = x_{\varepsilon}$, and V' is the derivative $dV^{-}(x)/dx$, evaluated at x_{ε} , and z_{ε} is defined below.

$$\sigma_{\rm DA}(n,\,\varepsilon) \propto \frac{\Gamma(x_{\varepsilon})}{V'(x_{\varepsilon})} |\chi_n(z_{\varepsilon})|^2 {\rm e}^{-\rho}$$
 (13)

$$V^{-}(x_{\varepsilon}) - V(x_{\varepsilon}) = \varepsilon \tag{14}$$

This x_{ε} serves as a point from which the separation between the products of the electron dissociation attachment, R' and X⁻, begins along the repulsive curve $V^{-}(x)$.

The x-dependent electronic energy of an RX' anion which can re-emit the electron is frequently described via a complex-valued potential W(x), eqn. (15), where the $i\Gamma(x)/2$ takes into account the electron re-emission.

$$W(x) = V^{-}(x) + i\Gamma(x)/2$$
 (15)

According to the Franck-Condon principle the vertical transition to a complex-valued potential W(x) as a result of a collision with an electron of energy ε , occurs at a z_{ε} which is a complex-valued x that satisfies eqn. (16).

$$W(z_{\varepsilon}) - V(z_{\varepsilon}) = \varepsilon \tag{16}$$

Upon expansion of W-V in powers of $z_{\varepsilon}-x_{\varepsilon}$ and using eqn. (16), one sees that z_{ε} is given by eqn. (17), where V'_{Δ} is given by eqn. (18).

$$z_{\varepsilon} = x_{\varepsilon} - i\Gamma/2V_{\Delta}' \tag{17}$$

$$V_{\Lambda}' = V^{-}(x_{\varepsilon}) - V'(x_{\varepsilon}) \tag{18}$$

[Equation (18) differs slightly from a value used in Refs. 19 and 21, where the $V'(x_{\varepsilon})$ did not appear. In that work attention was focused on the lowest vibrational state of the molecule, and $V'(x_{\varepsilon}) \cong 0$ there, and also $V^{-\prime}(x_{\varepsilon})$ is assumed to be very large.]

The $\exp(-\rho)$ in eqn. (13) is the probability (the survival probability)¹⁹⁻²² that a system formed on the $V^-(x)$ curve at x_{ε} will survive before re-emitting the electron, and so reach the intersection x_{ε} of the $V^-(x)$ and V(x) curves, eqn. (19), where $t_{\varepsilon}-t_{\varepsilon}$ is the time for separating R^++X^- system to go from the point of formation x_{ε} to the crossing point x_{ε} . In eqn. (19) $v_{\text{nuc}}(x)$ is the relative velocity of the separating nuclei at x. Beyond $x=x_{\varepsilon}$, the $V^-(x)$ curve is below V(x) [e.g., Fig. 1(a)] and the competing electron re-emission can no longer occur.

$$\rho = \int_{x_{\epsilon}}^{x_{c}} \frac{\Gamma \, \mathrm{d}x}{\hbar v_{\mathrm{nuc}}(x)} \equiv \int_{t_{\epsilon}}^{t_{c}} \frac{\Gamma \, \mathrm{d}t}{\hbar} \tag{19}$$

We see from eqn. (13) that the measurement of σ_{DA} as a function of ε and of the vibrational quantum state n provides information indirectly on $V^-(x)$ and on Γ . A simple modification of eqn. (13), namely eqn. (20) below, yields $\sigma_{DA}(T,\varepsilon)$, which can be compared with data on this quantity. One can, of course, obtain this σ_{DA} from $\sigma_{DA}(n,\varepsilon)$ by averaging the latter over the thermal distribution of n. The modification is to use, for this thermally averaged $|\chi_n|^2$, a statistical mechanical expression, which we have derived as an extension (to a complex-valued coordinate) of an expression⁴⁹ well-known for real coordinates, where Re and Im denote 'real part of' and 'imaginary part of', and are given in eqn. (17), and where $\Theta = \tanh(\hbar\omega\beta/2)$.

(13)
$$\langle |\chi_n(z_{\varepsilon})^2| \rangle_{av} = \left(\frac{\Theta \mu \omega}{\hbar \pi}\right)^{1/2}$$

(14) $\times \exp[(-\Theta(\operatorname{Re} z_{\varepsilon})^2 + (\operatorname{Im} z_{\varepsilon})^2/\Theta)(\mu \omega/\hbar)]$
ation (20)

Equation (20) was derived using Mehler's formula^{50,51} for sums of products of Hermite polynomials of different arguments, here z_{ε} and z_{ε}^* ; ω is the angular vibration frequency of the vibration $(\omega/2\pi = v)$, $\beta = 1/k_BT$, and μ is the reduced mass for the vibrational coordinate x. At low temperatures the exponent in eqn. (20) reduces to the value appropriate to the square of the amplitude of the wavefunction $\chi_o(z_{\varepsilon})$ of the lowest vibrational quantum state of this harmonic oscillator. The dependence of the initial value of $v_{\text{nuc}}(x)$ in eqn. (19) on the state n for a given ε was neglected in deriving eqn. (20) for these steep $V^{-}(x)$ values, an approximation was also made¹⁹ in the limiting form of a derivation leading to eqn. (13), through the use of a delta function of $x-z_{\varepsilon}$ as a final vibrational state wavefunction. Using an approximation, namely that the effective ω becomes temperature-dependent, one could extend eqn. (20) to anharmonic oscillators, as will be discussed elsewhere, together with giving a physically intuitive description of eqn. (13), including the proportionality constant, and an application of the equations to the data, so as to determine trends in slope of the anion potential energy curve $dV^-(x_{\varepsilon})/dx_{\varepsilon}$.

Summary

Vertical attachment energies $E_{\rm v}$ can be used to estimate thermal dissociative attachment energies $E_{\rm a}$, as in Table 2 for the case treated in Fig. 1(a). A treatment which contains a small attractive term for the anion potential energy function $V^-(x)$ was seen to provide a better agreement with experiment than one having only the purely repulsive term. The elastic, inelastic and thermal dissociative attachment cross-sections provide, indirectly, more detailed information on $V^-(x)$. Some of the underlying theory is discussed, eqn. (20) is derived, and the need for further *ab initio* calculations of $V^-(x)$ is noted.

Acknowledgements. It is a pleasure to acknowledge the support of this research by the National Science Foundation and by the Office of Naval Research. I am especially pleased to dedicate this article to Professor Lennart Eberson, on the occasion of his sixty-fifth birthday.

References

- 1. Eberson, L. Electron Transfer Reactions in Organic Chemistry, Springer-Verlag, New York 1987.
- 2. Savéant, J.-M. Adv. Phys. Org. Chem. 26 (1990) 1.
- 3. Shaik, S. S., Schlegel, H. B. and Wolfe, S. Theoretical Aspects of Physical Organic Chemistry. The S_N2 Mechanism, Wiley-Interscience, New York 1992.
- 4. Albery, W. J. Ann. Rev. Phys. Chem. 31 (1980) 277.
- 5. Domcke, W. Phys. Rep. 208 (1991) 97.
- 6. Christophorou, L. G., Ed. *Electron–Molecule Interactions* and their Applications, Academic Press, New York 1984, Vols. 1 and 2.
- 7. Burrow, P. D., Gallup, G., Fabrikant, I. I. and Jordan, K. D. Aust. J. Phys. 49 (1996) 23.
- 8. Chutjian, A., Garscaddin, A. and Wadehra, J. M. *Phys. Rep. 264* (1996) 393.
- 9. Chen, E. C. M., Albyn, K., Dussach, L. and Wentworth, W. E. J. Phys. Chem. 93 (1989) 6827.
- 10. Savéant, J.-M. J. Am. Chem. Soc. 109 (1987) 6788.
- 11. Krzysztofowicz, A. M. and Szmytkowski, C. J. Phys. B 28 (1995) 1593.
- 12. Guerra, M., Jones, D., Distefano, G., Scagnolari, F. and Modelli, A. J. Chem. Phys. 94 (1991) 484.
- 13. Shi, X., Chan, V. K., Gallup, G. A., and Burrow, P. D. J. Chem. Phys. 104 (1996) 1855.
- 14. Modelli, A., Scagnolari, F., Distefano, G., Guerra, M. and Jones, D. Chem. Phys. 145 (1990) 89.

- 15. Modelli, A., Scagnolari, F., Distefano, G., Jones, D. and Guerra, M. J. Chem. Phys. 96 (1992) 2061.
- 16. Burrow, A., Modelli, A., Chiu, N. S. and Jordan, K. D. J. Chem. Phys. 77 (1982) 2699.
- 17. Pearl, D. M. and Burrow, P. D. J. Chem. Phys. 101 (1994) 2940.
- 18. Wentworth, W. E., George, R. and Keith, H. J. Chem. *Phys.* 51 (1969) 1791.
- 19. O'Malley, T. F. Phys. Rev. 150 (1966) 14.
- 20. Bardsley, J. N., Herzenberg, A. and Mandl, F. *Proc. Phys. Soc.* 89 (1966) 321.
- 21. O'Malley, T. F. Phys. Rev. 155 (1967) 59.
- 22. Bardsley, J. N. J. Phys. B Ser. 2, 1 (1968) 349.
- 23. Herzenberg, A. J. Phys. B Ser. 2, 1 (1968) 548.
- 24. Birtwistle, D. T. and Herzenberg, A. J. Phys. B 4 1971) 53.
- 25. Dube, L. and Herzenberg, A. Phys. Rev. A 20 (1979) 194.
- 26. Yelets, I. S. and Kazansky, A. K. Sov. Phys. JETP 53 (1981) 499.
- 27. Yelets, I. S. and Kazansky, A. K. Sov. Phys. JETP 55 (1982) 258.
- 28. Kazansky, A. K. J. Phys. B 16 (1983) 2427.
- 29. Kazansky, A. K. and Yelets, I. S. J. Phys. B 17 (1984) 4767.
- 30. Kalin, S. A. and Kazansky, A. K. J. Phys. B 23 (1990) 4377.
- 31. Fabrikant, I. I. J. Phys. B 24 (1991) 2213.
- 32. Fabrikant, I. I. J. Phys. B 27 (1994) 4325.
- 33. Hahndorf, I., Illenberger, E., Mehr, L. and Manz, J. Chem. Phys. Lett. 231 (1994) 460.
- 34. Lehr, L. and Miller, W. H. Chem. Phys. Lett. 250 (1996) 515.
- 35. Lehr, L., Manz, J. and Miller, W. H. Chem. Phys. 214 (1997) 301.
- 36. Taylor, J. R. Scattering Theory, Wiley, New York 1972, p. 412.
- 37. Smith, K. H. The Calculation of Atomic Collision Processes, Wiley-Interscience, New York 1971, pp. 42-43.
- 38. Drukarev, G. F. Collisions of Electrons with Atoms and Molecules, Plenum, New York 1987, p. 46.
- 39. Wigner, E. P. Phys. Rev. 73 (1948) 1002.
- 40. Dojahn, J. G., Chen, E. C. M. and Wentworth, W. E. J. Phys. Chem. 100 (1996) 1949.
- 41. Gertitschke, P. L. and Domcke, W. Z. Phys. D 31 (1994) 171.
- 42. Fabrikant, I. L. Phys. Rev. A 43 (1991) 3478.
- 43. Bardsley, J. N. and Wadehra, J. M. J. Chem. Phys. 78 (1983) 7227.
- 44. Bardsley, J. N. and Wadehra, J. M. Phys. Rev. A 20 (1979) 1398.
- 45. Teillet-Billy, D, Malegat, L. and Gayuacq. J. P. J. Phys. B 20 (1987) 3201.
- 46. Fabrikant, I. I., Kalin, S. A. and Kazansky, A. K. J. Phys. B 25 (1992) 2885.
- 47. Pearl, D. M., Burrow, P. D., Fabrikant, I. I. and Gallup, G. A. J. Chem Phys. 102 (1995) 2737.
- 48. Fano, U. Phys. Rev. 124 (1961) 1866.
- 49. Feynman, R. P. Statistical Mechanics, Benjamin, Reading, MA 1972, pp. 50-51.
- 50. Erdelyi, A., Ed., Higher Transcendental Functions, Vol. 2, McGraw-Hill, New York 1953, pp. 194, eqn. (22).
- 51. Markham, J. J. Rev. Mod. Phys. 31 (1959) 956, eqn. (9.4). Received January 2, 1998.